MVA'98 IAPR Workshop on Machine Vision Applications, Nov. 17-19, 1998, Makuhari, Chiba, Japan

13—13

XR-US Data Fusion for Non-destructive Evaluation of Steel Components

M.Ancis, A.Campus, D.D.Giusto, and F.Tintrup

Dept. of Electrical and Electronic Engineering
University of Cagliari, Italy

Abstract

The paper aims at presenting a framework for visual inspection and defect detection of steel pipe welds in chemical and nuclear power plants.
Pipe welds are examined by means of X-ray (XR) and ultrasound (US) sensors; collected data are separately processed in order to extract features used in the fusion phase to detect and measure possible defects.
Results obtained on real images are presented and discussed.

1. Introduction

The aim of our study was to develop an automated tool for visual inspection of cooling pipes (in particular, the relevant welds) in nuclear power and chemical plants, exploiting X-rays and ultrasound sensor data.
This inspection is of fundamental importance for the sake of plant security, as well as for management aspects, since the missing substitution of a defected pipe may result in an environmental catastrophe, while the wrong substitution of a pipe in a good condition causes a notable increase in exercise expenses.
For the inspection, two of the main non-destructive technologies were chosen: X-rays and ultrasounds. These technologies show different characteristics, and their combined use may offer a more complete vision of the examined sample; in practice, they control the same scene under two different point of view.
In order to better exploit these complementary data, a fusion procedure has been implemented, allowing for a precise detection of defects in the weld under examination.
The data processing and fusion procedure that was developed is able to locate surface and inner defects, with a higher degree with respect to the separate use of the two inspecting techniques.

Address: DIEE, Piazza d'Armi, Cagliari 09123 Italy
E-mail: giusto@diee.unica.it
Homepage: http://www.diee.unica.it

2. XR data processing

XR images are processed in order to detect and characterize defects, if any, so that they can be evaluated in terms of the danger they may cause.
The first step is aimed at segment a scene into its different regions, and it is realized through an edge-detection filter; in particular, the Canny filter is used [1], as it allows a good identification of discontinuities, their precise localization, and a single filter response in presence of a single edge. It is based on the first derivative of a windowed Gaussian function:

$$G = \begin{cases} \exp\left\{\left(-1/\sigma^2\right)\left(x^2+y^2\right)\right\} & (x,y)\in[-W/2, W/2] \\ 0 & elsewhere \end{cases}$$

where W is the window size, and σ^2 is the variance of the Gaussian function.
The optimum filter for a given $\boldsymbol{n}$ direction is defined as:

$$Gn = \partial G/\partial \boldsymbol{n} = \boldsymbol{n}\cdot\nabla G$$

The mathematical condition indicating that a point is belonging to an edge is:

$$\frac{\partial}{\partial \boldsymbol{n}} Gn * I = 0$$

where I is the image, and * is the convolution operator.
This relation can be rewritten as:

$$\frac{\partial^2}{\partial \boldsymbol{n}^2}(G * I) = 0$$

Moreover, it is possible to have an estimation of the edge strength by the following quantity:

$$\left|Gn * I\right| = \left|\nabla(G * I)\right|$$

A crucial step in applying this filter to an image lies in the determination of the variance, which reflects in the results' quality. Another important point is the definition of two thresholds for the hysteresis effect in tracing the edges. The values heuristically determined for XR data are reported in the Results' section.
Using the edge map so obtained, and the original data, a scene is transformed into a binary image, where pixels are divided into background and objects that may be defects.
The binarization is achieved through a procedure based on the method proposed in [2,3]. In particular, a thresholding surface is obtained by interpolating the gray

values of pixels belonging to each object's edge, and a threshold value is assigned to each image pixel.

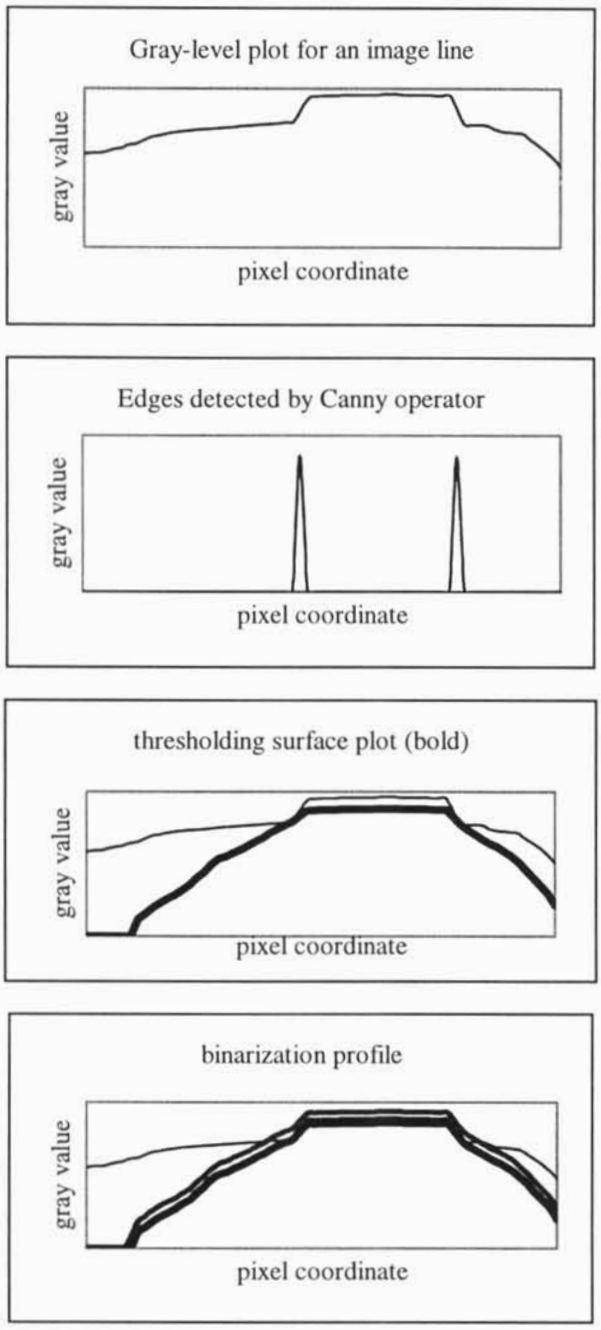

Fig.1. An example of thresholding surface identification and binarization profile for XR data.

There exist several approaches aimed at interpolating a set of given points. In this case, the Laplacian of the thresholding surface is used, defined as

$$L(S)=\frac{\partial^2 S}{\partial x^2}+\frac{\partial^2 S}{\partial y^2}$$

and it is set to zero at first. The thresholding surface is set at first as:

$$S(x,y)=\begin{cases} I(x,y) & \text{if } (x,y) \text{ is an edge} \\ 0 & \text{elsewhere} \end{cases}$$

For each image pixel, the discrete Laplacian value is computed by convolving the image with the following kernel:

$$\begin{bmatrix} 0 & 1 & 0 \\ 1 & -4 & 1 \\ 0 & 1 & 0 \end{bmatrix}$$

In such a way it is possible to compute the residual $R(x,y)$, which is used, after appropriate weighting, to update the gray values of the thresholding surface in points not belonging to edges. The updating formula is:

$$S(x,y) \leftarrow S(x,y)+\beta\, R(x,y)/4$$

where the value for β is between 1 and 2.

The residual value is decreasing with each iteration; the procedure is stopped when the maximum residual value is under a predefined threshold.

At the end of this interpolation process, a thresholding surface is obtained that is able to segment an image into defects and background, if the point-to-point difference, in absolute value, is under a given threshold. Figures 1, 2, and 3 present an example of this procedure for a 1D case.

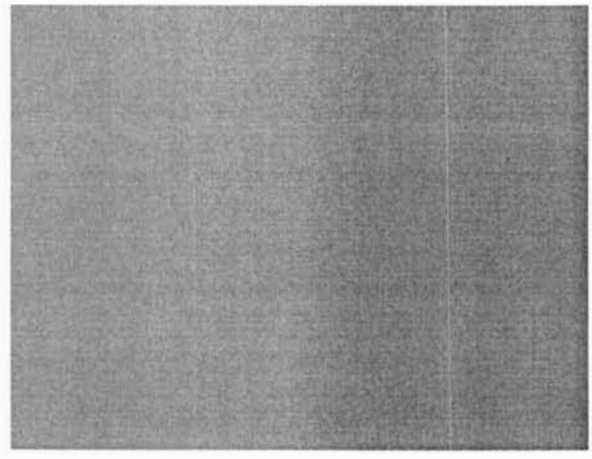

Fig.2. Original XR data.

After binarization, images are processed by a median operator, in order to filter away noisy pixels (the size of the neighborhood is set to 3×3).

The final image is then used for feature extraction and object characterization, towards the final goal of defect detection.
In particular, the following features are measured for each connected object: barycentre coordinates, area, elongation, elongation direction. The last two features are measured using the minimum bounding rectangle.
These object features are used together with those obtained by processing the US data, in the final defect detection step by data fusion.

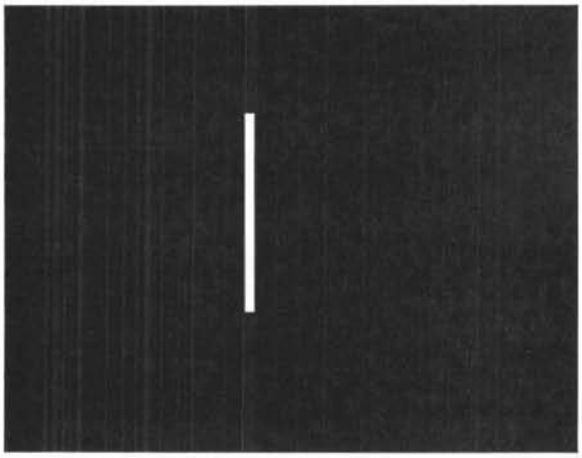

Fig.3. Binarized XR data.

3. Ultrasound data processing

Ultrasound data are acquired using the A-scan mode, which allows to represent along the y axis the echo amplitude of the emitted signal, while along the x axis reports the signal travel time.
Figure 4 shows an example of A-scan output.

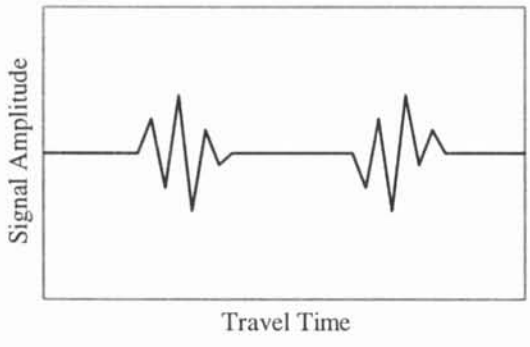

Fig.4. An example of A-scan.

The presence of the left group of peaks and valleys indicates a discontinuity, i.e. a step-edge between different materials (that means the change of acoustic properties). The right group indicates the opposite discontinuity.
US data are structured as voxels, that is, as a 3D matrix where (x, y) represent the coordinates of the sensor on the material surface, and z represent the travel time.
By fixing (x, y), a single A-scan is obtained. By fixing z, a slice is extracted from the 3Ddata, representing the situation at a certain depth; this information is used to localize the defect in (x, y, z); in fact, this is the way the localization may be carried out, as XR data give only information about (x, y), that means that it is cumulative along the z direction.
US data are 2D processed through the use of macro-slices; as the thickness of a single slice is just in the range of tens of micrometers, macro-slices are extracted by fusing together some slices. An example of macro-slice is given in Figure 5.
In order to extract macro-slice objects that may belong to a defect, macro-slices are then binarized in a simple way, without using complex edge detectors.

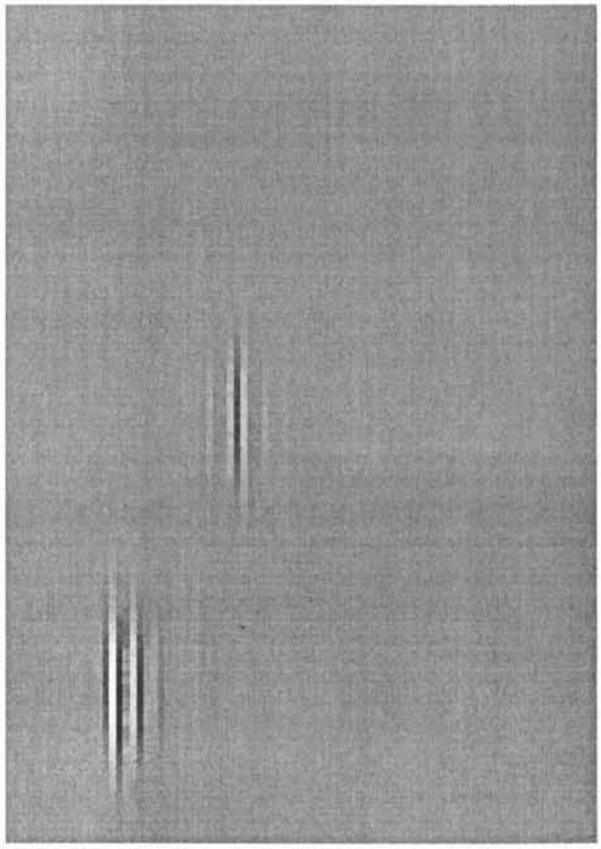

Fig.5. An example of macro-slice.

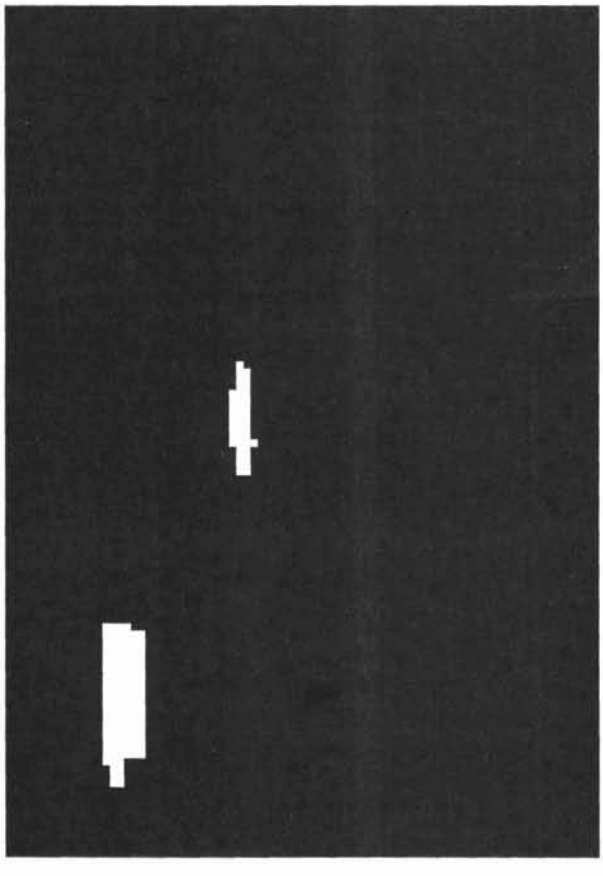

Fig.6. The binarization process applied to a macro-slice.

In fact, macro-slice objects are extracted by just evaluating the difference between each pixel value and the value corresponding to the absence of signal echo (in the present case, this value is 128); if this difference, in absolute value, is above a certain threshold, the pixel is labeled as macro-slice object, otherwise as background. The result of this operation is presented in Figure 6.
Macro-slice objects are then characterized by features extracted from the previous pair of images; in particular, these features are: barycentre coordinates, area, elongation, elongation direction, depth range.
With respect to XR data, US data are able to locate an object in a 3D space; on the other end, the information they furnish about size and shape are quite less accurate.
At this point, after processing all the macro-slices, a reduction in the amount of data is necessary, as a 3D object may be divided into several macro-slice object. This is done by merging together macro-slice objects that are adjacent; the merging strategy is based on the spatial adjacency of a pair of macro-slice objects, determined on the basis of barycentre coordinates and depth ranges.

4. Data fusion and defect detection

The last processing step is then related to fuse all the information regarding the objects found in XR and US data, aiming at detecting defects in the welds.
The fusion is implemented as a matching procedure, based on the features measured for each object in XR/US binarized data. A matrix is defined whose elements are the results of a function applied to the object features. This function takes as input these features, and outputs a minimum value when these features belong to a same defect. By analyzing this matrix is possible to operate a match between XR and US data.
The function used in defining the matrix is the following:

$$f(x_{XR}, x_{US}, y_{XR}, y_{US}, \theta_{XR}, \theta_{US}) = |x_{XR} - x_{US}| + |y_{XR} - y_{US}| + |\theta_{XR} - \theta_{US}|$$

where (x_{XR}, y_{XR}) are the barycentre coordinates of an object in XR data, (x_{US}, y_{US}) are the barycentre coordinates of an object in US data, θ_{XR} and θ_{US} are the elongations of an object in XR and US data, respectively.
After this matching phase, objects become more complex and the set of measures complete and precise, and defects can be finally detected and fully characterized; each defects is also associated to a certainty factor, as in some cases, defects may be detected by just a set of features, coming either from XR or US data.

Acknowledgments

This paper reports on work carried out by the authors within the MISTRAL project, funded by the European Union (Brite-Euram programme; contract n. CT96-0310). The experimental data presented in the paper were furnished by EDF-DER, Chatou, France.

References

1. J.Canny, "A computational approach to edge detection," IEEE Transactions of Pattern Analysis and Machine Intelligence, vol. 8, no. 6, pp. 679-698, 1986.
2. S.D.Yanowitz, and A.M.Bruckstein, "A new method for image segmentation," Computer Graphics and Image Processing, vol. 46, pp. 82-95, 1989.
3. A.K.Jain, and M.-P.Dubuisson, "Segmentation of X-ray and C-scan images of fiber reinforced composite materials," Pattern Recognition, vol. 25, no. 3, pp. 257-270, 1992.